






Article

A Review and Mathematical Treatment of Infinity on the Smith Chart, 3D Smith Chart and Hyperbolic Smith Chart

María Jose Pérez-Peñalver ¹, Esther Sanabria-Codesal ¹, Florica Moldoveanu ²,
Alin Moldoveanu ^{2,*}, Victor Asavei ², Andrei A. Muller ³ and Adrian Ionescu ³

¹ Universitat Politècnica de València, Matemática Aplicada, 46022 Valencia, Spain; mjperez@mat.upv.es (M.J.P.-P.); esanabri@mat.upv.es (E.S.-C.)

² Department of Computer Science and Engineering, Faculty of Automatic Control and Computers, University POLITEHNICA of Bucharest, 060042 Bucharest, Romania; florica.moldoveanu@cs.pub.ro (F.M.); victor.asavei@cs.pub.ro (V.A.)

³ Ecole Polytechnique Federale de Lausanne, Nanoelectronic Devices Laboratory, 1015 Lausanne, Switzerland; andrei.muller@epfl.ch (A.A.M.); adrian.ionescu@epfl.ch (A.I.)

* Correspondence: alin.moldoveanu@cs.pub.ro

Received: 3 September 2018; Accepted: 28 September 2018; Published: 2 October 2018



Abstract: This work describes the geometry behind the Smith chart, recent 3D Smith chart tool and previously reported conceptual Hyperbolic Smith chart. We present the geometrical properties of the transformations used in creating them by means of inversive geometry and basic non-Euclidean geometry. The beauty and simplicity of this perspective are complementary to the classical way in which the Smith chart is taught in the electrical engineering community by providing a visual insight that can lead to new developments. Further we extend our previous work where we have just drawn the conceptual hyperbolic Smith chart by providing the equations for its generation and introducing additional properties.

Keywords: hyperbolic geometry; Möbius transformation; Smith chart

1. Introduction

The 2D Smith chart, one of the most helpful and recognized microwave engineering tools, was proposed by Philip H. Smith in 1939 [1] and further developed by the same author throughout the years [2] before becoming an icon of high frequency engineering [3,4]. Starting the last decades of the 20 century it became used widely in major computer aided design CAD/testing tools as add on but also as a key part in stand-alone tools [5,6]. The Smith chart is bounded within the unit circle of the reflection coefficient's plane and provides by its practical size an excellent visual approach of the microwave problems [1,6]. But it also has some disadvantages, such as that loads with voltage reflection coefficient magnitude exceeding unity cannot be represented in a practical compact size. These loads appear in active circuits exhibiting negative resistance or in circuits with complex characteristic impedance and can be represented in 2D by constructing an additional reciprocal negative Smith chart [2]. However, the Smith chart and the negative Smith chart cannot be used in a unitary way in the same time since the scales used are different. The 3D Smith chart representation [7] using the Riemann sphere and the circle conserving property of Mobius transformations on it lead to the creation of the first 3D Smith chart tool which combines the design of active and passive components on the unit sphere. The reason for seeking a 3D embedded generalization was motivated by the aspiration to have a single compact chart proper for dealing with negative resistance impedances without distorting the circular shapes of the Smith chart, thus keeping its properties. Described in References [7–10], the 3D Smith chart has

its roots in the group theory of inversive geometry [11] where the point at infinity seen as a pole on a sphere plays a key role.

However, the 3D Smith chart has some inconveniences, for example it cannot be easily used without a software tool, while the idea of using a 3D embedded surface may be still discouraging for the electrical engineering community which is used to the 2D Smith chart [12]. In References [13,14] we proposed a rather arts based hyperbolic geometry model dealing with all the reflection coefficients within the unit disc.

In this article, we present the geometrical treatment of infinity on the 2D Smith chart, 3D Smith chart and further develop the equations and properties of the intuitive hyperbolic Smith chart drawing [13,14]. This is done by using the Kleinian view of geometry, that is, infinity treatment of Möbius transformations [11,15] for the 2D and 3D Smith chart and basic elements of pure Non-Euclidean geometry [16–18] for the hyperbolic Smith chart.

2. Planar Smith Chart and Möbius Transformations

The relation between the normalized impedance $z = Z/Z_0 = r + jx$ and the voltage reflection coefficient ρ is given by [1,2,7,19]:

$$\rho = \frac{z - 1}{z + 1}, z \neq -1 \quad (1)$$

The expression (1) maps the impedances with positive normalized resistance r (belonging to the right half plane (RHP)) into the limited area of the unit circle and the impedances with negative resistance are projected outside the unit circle, as we observe in Figure 1:

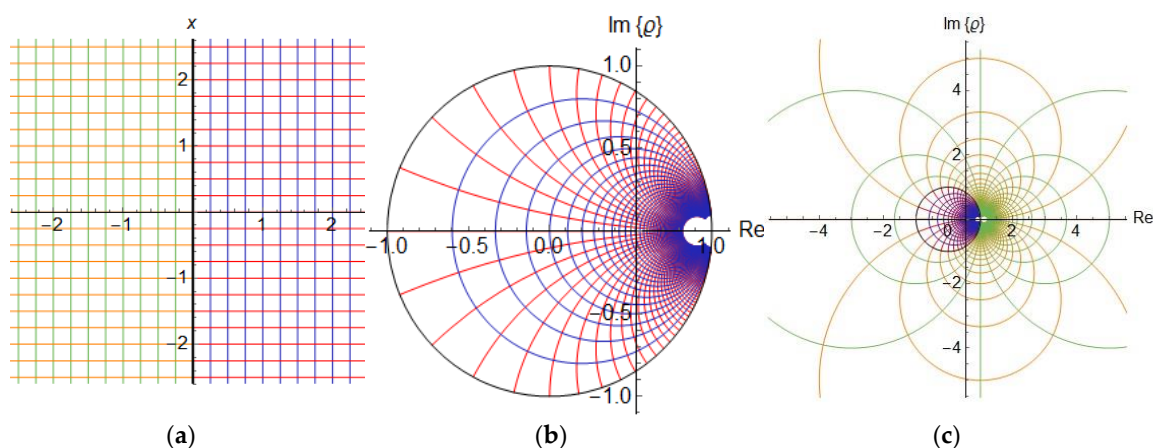


Figure 1. (a) Normalized grid of the impedance plane; (b) Smith chart (voltage reflection coefficients plane); (c) extended Smith chart including negative resistance impedances voltage reflection coefficient representations too, infinite values are thrown in all directions of the 2D plane.

The transformation (1) regarded throughout the references [1–6] and [12,19] as “conformal transformation”, “bilinear map” or “Möbius transformation” is from a geometrical perspective a very simple direct inversive transformation [8,9,11,15]. Direct inversive transformations are defined by (2) and together with the transformations defined by (3) (indirect inversive) they form the group of inversive transformations [8,15].

$$T(z) = \frac{az + b}{cz + d} \quad (2)$$

$$TI(z) = \frac{a\bar{z} + b}{c\bar{z} + d} \quad (3)$$

Both (2) and (3) are conformal transformations and surely (1) is a particular case of (2). The geometry of these transformations can be educationally explored by placing instead of z a photo:

Applying transformations of type (2) to Figure 2a we can see in both Figure 2b,c that the transformation (2) maps always lines like shapes into circle arcs [8] (contour of the photo) (their position and length being dependent on the placement of (a) in the complex plane). This is an innate property of the Möbius transformations but depending on the photo position in the normalized plane, points can be sent towards infinity. In Figure 2b we can notice that points are already thrown outside of the unite circle since the position of the photo in Figure 2a was not completely in the right half plane of the z plane RHP. Möbius transformations as all inversive transformations do not always map circles into circles and lines into circles on a 2D sheet since points can be thrown not only far from the unit circle but also at infinity [7,15].

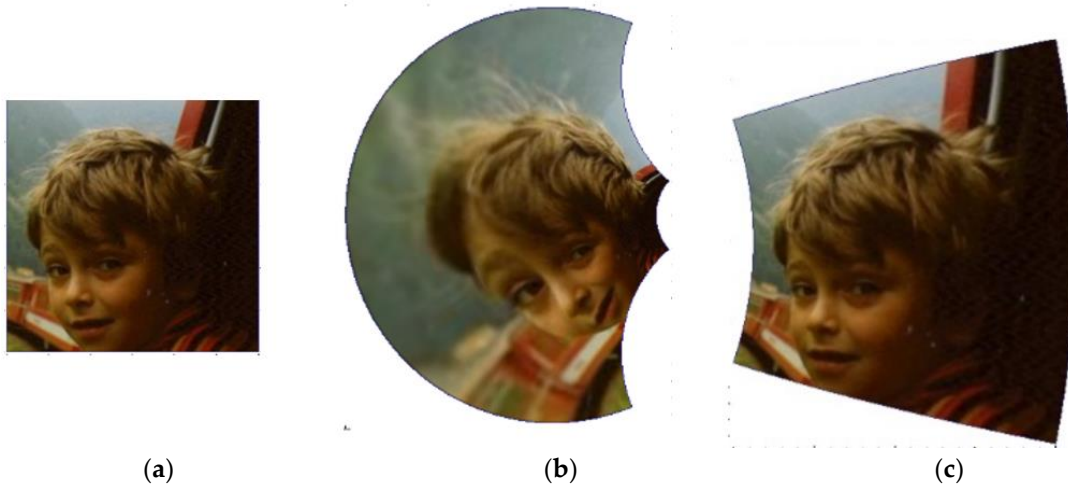


Figure 2. (a) a photo of Andrei in the impedance plane; (b) mapping of (1) applied to the photo; (c) mapping of (2) considering $a = 1, b = -1, c = 1, d = 5$.

If we extended the Möbius transformation (1) such that

$$M(z) = \rho = \frac{z-1}{z+1}; M(-1) = \infty; M(\infty) = 1, \quad (4)$$

then we have a map between the z -plane and the ρ -plane. A ρ -plane point in terms of the load normalized resistance r and reactance x , is given by:

$$M(z = r + jx) = \frac{r^2 + x^2 - 1}{(r+1)^2 + x^2} + j \frac{2x}{(r+1)^2 + x^2}, \quad (5)$$

then the z -plane circumference $|z| = 1$ is sent to the ρ -plane imaginary axis. Its inverse, $M^{-1}(\rho) = z$ is

$$M^{-1}(\rho = \rho_r + j\rho_x) = \frac{1 + \rho}{1 - \rho} = \frac{1 - \rho_r^2 - \rho_x^2}{(1 - \rho_r)^2 + \rho_x^2} + j \frac{2\rho_x}{(1 - \rho_r)^2 + \rho_x^2}; \rho \neq 1, \quad (6)$$

then $M^{-1} : \mathbb{C} \setminus \{1\} \rightarrow \mathbb{C} \setminus \{-1\}$; $M^{-1}(1) = \infty$; $M^{-1}(\infty) = -1$ is the inverse in the extended complex plane map.

The typical flat 2D Smith chart only considers the $|\rho| \leq 1$ region. Infinity on a 2D Smith chart embedded on a planar surface means Figure 1 which makes it difficult to use when loads with negative resistance occur. Facing this problem, Maxime Bocher, a student of Felix Klein and president of the American Mathematical Society, proposed in Reference [11] the general solution for all Möbius transformations and indirect inversive transformations, so that these should always map circles into circles or lines into circles.

3D Smith Chart and Infinity

To construct the 3D Smith chart [7–10] we place the extended Smith chart inside the equatorial plane of the Riemann sphere (Figure 3) and using the south pole we map it on the unit sphere (Figure 4):

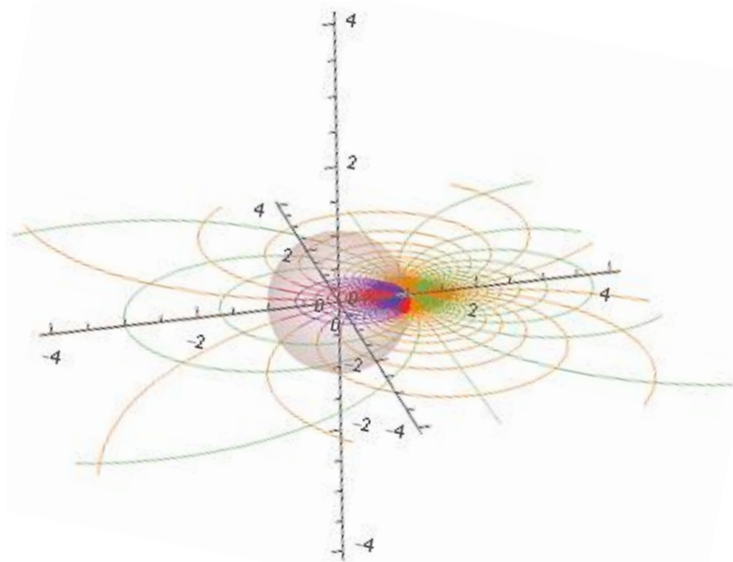


Figure 3. Extended Smith chart (Figure 1c) placed on the equatorial plane of the Riemann sphere, before its mapping on the sphere via the south pole.

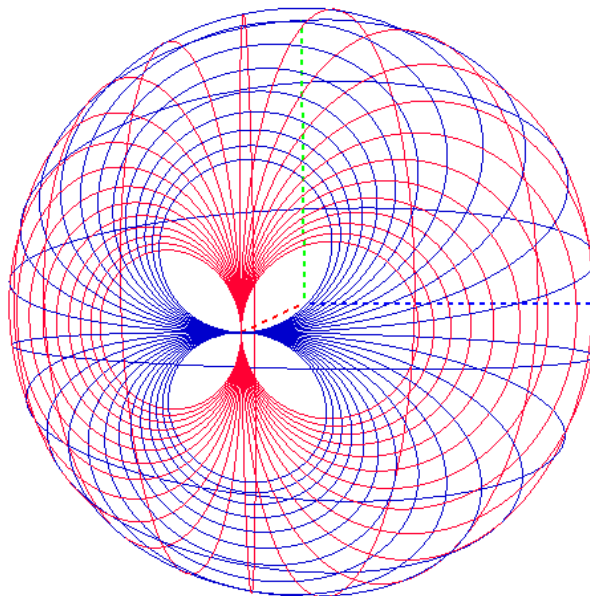


Figure 4. 3D Smith chart obtained with the 3D Smith chart Tool [20], infinity of the voltage reflection is the South pole, circle shape of the Smith chart is preserved.

The 3D Smith chart [20] obtained in Figure 4 has a variety of convenient attributes analogous to a real Earth globe, as can be summarized in Table 1.

Table 1. Comparative capabilities of Smith and 3D Smith charts.

Comparative Capabilities	Smith Chart	3D Smith Chart
Positive resistance	Interior of unity circle	North hemisphere
Negative resistance ($ \rho > 1$)	NO (towards infinity)	South hemisphere
Perfect match	Origin	North pole
$ \rho = \infty$	NO	South pole
Inductive	Above the abscissa	East
Capacitive	Below the abscissa	West
r,x,g,b constant	Circles, circle arcs, 1 line	Circles
Purely resistive	Abscissa	Greenwich meridian
Power levels/group delays	NO	3D space(Exterior > 0 , Interior < 0)

In Figure 5 we can see the idea of infinity more humanly. A girl and a boy start from the centre of the chart moving on the ordinate of the reflection plane ($r = 0$). When they reach the contour ($|\rho| = 1$), their journey ends and they can never meet again (and just imagine meeting again at infinity). On the 3D Smith chart, once they reach the equator they can continue walking on the same great circle and still meet at infinity (south pole) which is compact and reachable.

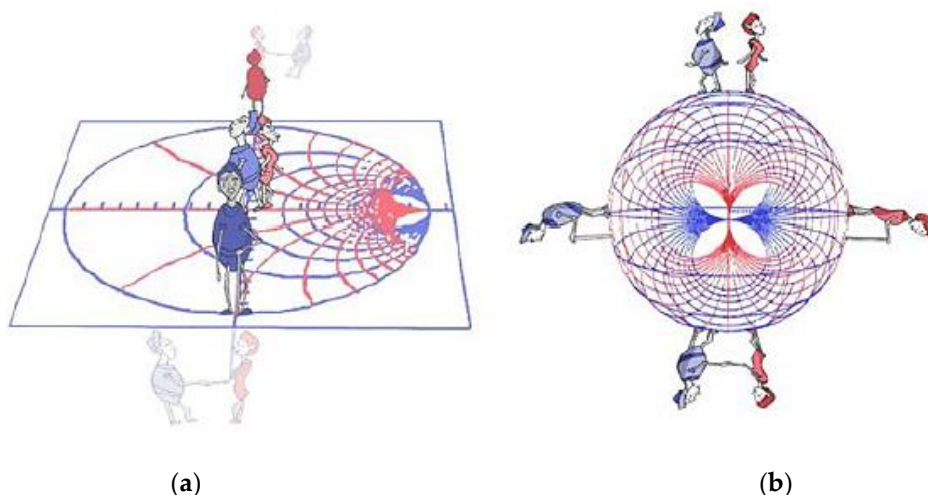


Figure 5. Intuitive representation of infinity on the 2D Smith chart (a) and 3D Smith chart; (b) South pole-image of infinite voltage reflection coefficient (magnitude) [20].

We consider the stereographic projection, by using the south pole $S = (0, 0, -1)$, on the complex plane $\pi_S : \mathbb{S} \setminus \{S\} \rightarrow \mathbb{C}$, where \mathbb{S} represent the surface of the unit sphere:

$$\pi_S(x_S, y_S, z_S) = \frac{x_S}{z_S + 1} + j \frac{y_S}{z_S + 1} \tag{7}$$

This transformation is a bijection and by applying the inverse to the ρ -plane, then the equations of the 3D Smith chart are presented by:

$$\rho^S(\rho = \rho_r + j\rho_x) = \left(\frac{2\rho_r}{|\rho|^2 + 1}, \frac{2\rho_x}{|\rho|^2 + 1}, \frac{1 - |\rho|^2}{|\rho|^2 + 1} \right) \tag{8}$$

In the same way, by applying first the Möbius transformation (1) and then ρ^S (8), we calculate the corresponding point in the 3D Smith chart of each point $z = r + jx$. This is just:

$$(\rho^S \circ M)(z = r + jx) = \left(\frac{|z|^2 - 1}{|z|^2 + 1}, \frac{2x}{|z|^2 + 1}, \frac{2r}{|z|^2 + 1} \right) \tag{9}$$

Conversely, a given point on the unit sphere $(x_S, y_S, z_S) \in \mathbb{S} \setminus \{S\}$ (i.e., $x_S^2 + y_S^2 + z_S^2 = 1$) is mapped to in the ρ -plane (i.e., the sphere equatorial plane) by:

$$\rho(x_S, y_S, z_S) = \pi_S(x_S, y_S, z_S) = \frac{x_S + jy_S}{z_S + 1} \tag{10}$$

Then, the reflection coefficient magnitude is connected to the coordinate z_S of the sphere and the phase of the reflection coefficient is equal to the angle of the point (x_S, y_S) with respect to the sphere x_S axis:

$$|\rho| = \sqrt{\frac{1 - z_S}{1 + z_S}}, \quad \varphi_\rho = \arctan\left(\frac{y_S}{x_S}\right) \tag{11}$$

Similarly, $(x_S, y_S, z_S) \in \mathbb{S} \setminus \{S\}$ is mapped into in the z -plane, considering $M^{-1}(6)$, by:

$$(M^{-1} \circ \rho)(x_S, y_S, z_S) = \frac{z_S + jy_S}{1 - x_S} \tag{12}$$

3. A Hyperbolic Smith Chart

Here we present the mathematical theory that lies behind the intuitive models that we have presented in References [13,14].

The extended complex ρ -plane (Figure 1c) includes also the loads outside the unit circumference $|\rho| = 1$ but thrown also towards infinity and the compact representation requires a sphere) (Figure 4), which necessitates a software tool for its practical use.

In this hyperbolic approach while maintaining a flat surface, we use models associated to the hyperbolic geometry, the Weierstrass Model and its stereographic projection onto the Poincaré unit disk in the plane [15].

We consider extended complex ρ -plane and map it onto the superior part of two sheet hyperboloid using the usual parametrization of this surface. Then, by using the stereographic projection from the upper sheet hyperboloid onto the unit disc $\mathbb{D} = \{\rho \in \mathbb{C} : |\rho| > 1\}$ (used in the Poincaré unit disc model of hyperbolic geometry), we construct the Hyperbolic Smith chart (Figures 6 and 7).

A generic ρ -plane point $\rho = \rho_r + j\rho_x = |\rho| e^{j\varphi_\rho}$ is mapped on

$$\mathbb{H}^+ = \left\{ (x_{\mathbb{H}}, y_{\mathbb{H}}, z_{\mathbb{H}}) \in \mathbb{R}^3 : x_{\mathbb{H}}^2 + y_{\mathbb{H}}^2 + z_{\mathbb{H}}^2 = -1, z_{\mathbb{H}} > 0 \right\}, \tag{13}$$

by the usual parametrization of this surface $t : \mathbb{C} \rightarrow \mathbb{H}^+$:

$$t(\rho = \rho_r + j\rho_x) = \left(\rho_r, \rho_x, \sqrt{1 + |\rho|^2} \right), \tag{14}$$

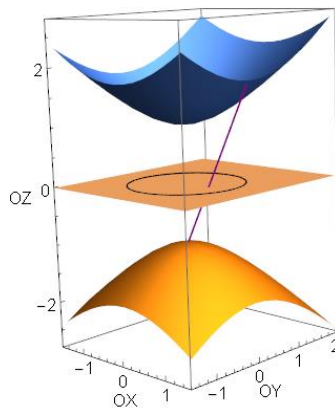


Figure 6. Relation between \mathbb{H}^+ and \mathbb{D} through stereographic projection s .

Next, by applying the stereographic projection $s : \mathbb{H}^+ \rightarrow \mathbb{D}$, from the point $(0, 0, -1)$, on the complex plane to a generic point in the space $(x_{\mathbb{H}}, y_{\mathbb{H}}, z_{\mathbb{H}}) \in \mathbb{H}^+$, we obtain that the point is mapped into the unit disc \mathbb{D} centered on the origin, as in the Figure 6:

$$s(x_{\mathbb{H}}, y_{\mathbb{H}}, z_{\mathbb{H}}) = \frac{x_{\mathbb{H}}}{z_{\mathbb{H}} + 1} + j \frac{y_{\mathbb{H}}}{z_{\mathbb{H}} + 1} \tag{15}$$

Therefore, the hyperbolic Smith chart equation in terms of the voltage reflection coefficients is given by:

$$\rho^h(\rho = \rho_r + j\rho_x) = (s \circ t)(\rho) = s\left(\rho_r, \rho_x, \sqrt{1 + |\rho|^2}\right) = \frac{\rho_r}{1 + \sqrt{1 + |\rho|^2}} + j \frac{\rho_x}{1 + \sqrt{1 + |\rho|^2}} \tag{16}$$

By arithmetical manipulations we can further get the connection to the resistance r and reactance x :

$$(\rho^h \circ M)(z = r + jx) = \frac{|z|^2 - 1}{(r+1)^2 + x^2 + \sqrt{2(1+|z|^2)((r+1)^2 + x^2)}} + j \frac{2x}{(r+1)^2 + x^2 + \sqrt{2(1+|z|^2)((r+1)^2 + x^2)}} \tag{17}$$

In Figure 7, we observe the different steps in the construction of the Hyperbolic Generalized Smith chart: First, the generalized Smith chart is sent by t (14) on the upper sheet of the hyperboloid and then the stereographic projection s (15) send it in the Poincaré unit disc model.

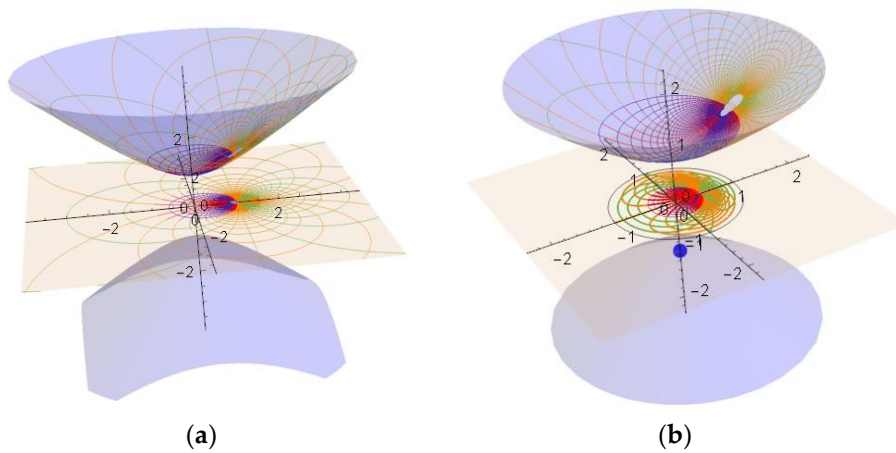


Figure 7. Steps in construction of the Hyperbolic Generalized Smith chart [13,14]: (a) Generalized Smith chart orthogonally projected on the upper part of the two-sheet hyperboloid (it spreads to infinity but on the upper sheet of the hyperboloid); (b) stereographic mapping from the upper hyperboloid on the 2D plane (Figure 6)—the infinity becomes the contour of the unit circle (from point $S = (0, 0, -1)$,—blue colour).

Conversely, a generic point $d = (x_h, y_h) \in \mathbb{D}$, in the unit disc centred on the origin, then, $d = x_h + jy_h = |d| e^{j\varphi_d}$, $|d| < 1$, is mapped through the inverse stereographic projection $s^{-1} : \mathbb{D} \rightarrow \mathbb{H}^+$, into a point in the upper hyperboloid:

$$s^{-1}(d = x_h + jy_h) = \left(\frac{2x_h}{1 - |d|^2}, \frac{2y_h}{1 - |d|^2}, \frac{1 + |d|^2}{1 - |d|^2} \right) \tag{18}$$

Next, this point in the upper hyperboloid is mapped into \mathbb{C} by applying the orthogonal projection $t^{-1} : \mathbb{H}^+ \rightarrow \mathbb{C}$. Therefore, a given generic point $d = (x_h, y_h)$ in the Hyperbolic Smith chart is mapped to the ρ -plane by:

$$\rho(d) = \rho^{h-1}(d) = (t^{-1} \circ s^{-1})(d) = \frac{2x_h}{1 - |d|^2} + j \frac{2y_h}{1 - |d|^2} \quad (19)$$

To find the expression in the z -plane, we need to consider (19) and the extended transformation $M^{-1}(6)$. Then:

$$z(d) = (M^{-1} \circ \rho^{h-1})(d = x_h + jy_h) = \frac{1 - 6|d|^2 + |d|^4}{(1 + |d|^2)((1 + |d|^2) - 4x_h)} + j \frac{4y_h(1 - |d|^2)}{(1 + |d|^2)((1 + |d|^2) - 4x_h)} \quad (20)$$

4. Properties

The Hyperbolic Smith chart has useful properties. In this section, we summarize them (Figure 8). The entire Smith chart is mapped into the interior of the 0.414 radius circle of the hyperbolic chart.

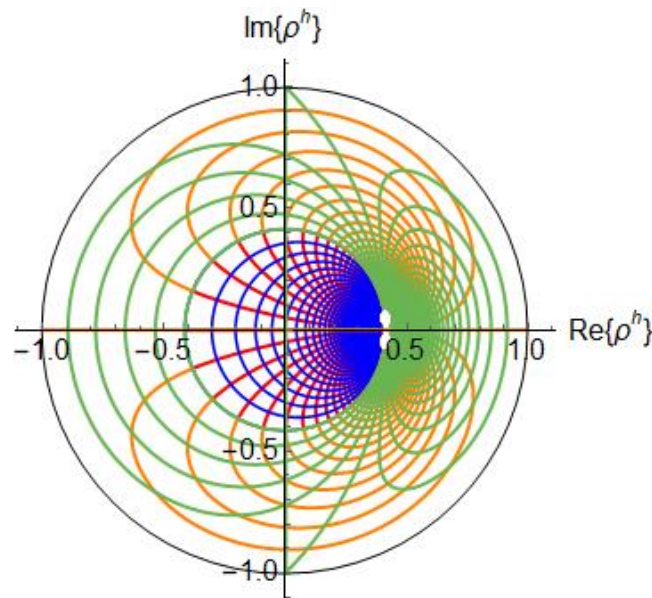


Figure 8. Hyperbolic Smith chart. Circuits with the magnitude of the voltage reflection coefficient below 1 are mapped into the interior of the 0.414 hyperbolic circle in ρ^h (the circuits with blue normalized resistance r and with red normalized reactance x) while the circuits with negative normalized resistance (green) are mapped in between the 0.414 radius circle and the unit circle (in this the constant normalized reactance circle are coloured in orange).

The circumference of radius one in the ρ -plane, $|\rho| = 1$, is mapped by (16) to the circumference of radius $\frac{1}{1 + \sqrt{2}} = \sqrt{2} - 1 \simeq 0.414$ in the ρ^h -plane, $|\rho^h| = 0.414$ and $|\rho^h| = 0$ in $|\rho^h| = 0$.

The Hyperbolic Smith chart contains the circuits with inductive reactance above the horizontal (real line) of the ρ^h -plane and the circuits with capacitive reactance below the real line of the hyperbolic reflection plane, like in the Smith chart. Further, as seen from (16), the constant reflection coefficients circles $0 \leq |\rho| \leq 1$ of the 2D Smith chart are projected onto circles with $0 \leq |\rho^h| \leq 0.414$ in the hyperbolic reflection coefficients plane. The $1 < |\rho| < \infty$ constant circles (which are exterior to the 2D Smith chart or in the South hemisphere on the 3D Smith chart) and which are important in active circuit design are contained in limited region of the hyperbolic reflection coefficients plane with $0.414 < |\rho^h| < 1$, as shown in Figure 9, and their circular forms is unaltered. The image of the

infinite magnitude constant reflection coefficient circle $|\rho| = \infty$ unimaginaire to represent even on a generalized 2D Smith chart becomes the contour of the new chart $|\rho^h| = 1$.

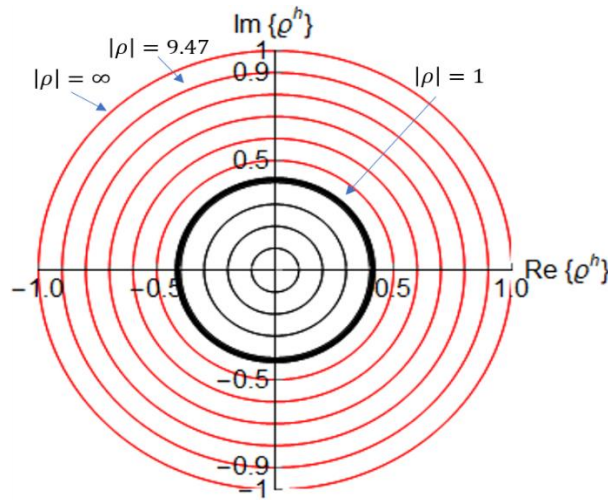


Figure 9. Hyperbolic Smith chart. Constant $0 < |\rho| < \infty$ contours are represented by circles on the Hyperbolic Smith chart and entirely mapped into the hyperbolic reflection coefficients plane $0 < |\rho^h| < 1$; $|\rho| = 0 \Leftrightarrow |\rho^h| = 0$; $|\rho| = 1 \Leftrightarrow |\rho^h| = 0.414$; $|\rho| = \infty \Leftrightarrow |\rho^h| = 1$ (in red are the $|\rho| > 1$ circles while in black the $|\rho| < 1$ circles). Thus, infinity of the magnitude of the reflection coefficient can be represented on the contour of the hyperbolic Smith chart (as in hyperbolic geometry) [15]

If we consider lines of constant resistance equal to k in the z -plane, $r = k$, we obtain in the ρ^h -plane the part inside of the unit circle of the quartic curve:

$$k(x_h^4 + 4x_h^3 + 2x_h^2(1 + y_h^2)) - x_h^4 + 6x_h^2 - 2x_h^2y_h^2 + 4kx_h(y_h^2 - 1) = 1 + y_h^4 - 6y_h^2 + k(1 + 2y_h^2 + y_h^4) \tag{21}$$

and in the same way if we consider lines of constant reactance $x = k$ in the z -plane we get in the ρ^h -plane the part inside of the unit circle of the quartic curve:

$$k(x_h^4 + 4x_h^3 + 2x_h^2(1 + y_h^2)) + 4x_h^2y_h^2 + 4kx_h(y_h^2 - 1) = 4y_h - 4y_h^2 - k(1 + 2y_h^2 + y_h^4) \tag{22}$$

as shown in Figure 10. These quartic curves are orthogonal along the curve in ρ^h -plane, corresponding to the image of the hyperbola $r^2 - x^2 = 1$ in the z -plane.

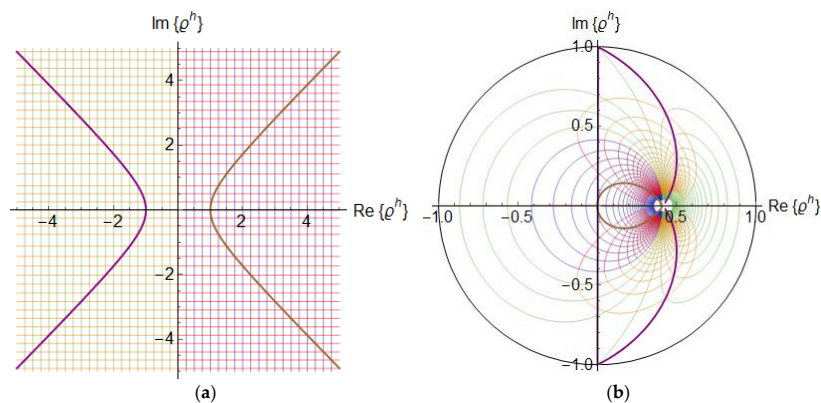


Figure 10. The (a) quartic curves are orthogonal in the (b) image of the points of the hyperbola $r^2 - x^2 = 1$ in the z -plane.

In the hyperbolic Smith chart, by using (19) we see that the reflection coefficient is:

$$|\rho| = \frac{2|d|}{1 - |d|^2}, \quad \varphi_\rho = \arctan\left(\frac{y_h}{x_h}\right) \quad (23)$$

We observe that the phase of the reflection coefficient is the same in the ρ -plane and the ρ^h -plane and the magnitudes are clearly related.

By using (20), we obtain that the normalized impedance is:

$$|z| = \frac{\sqrt{(1-6|d|^2+|d|^4)^2 + (4y_h(1-|d|^2))^2}}{(1+|d|^2)((1+|d|^2)-4x_h)} \quad (24)$$

$$\cot(\varphi_z) = Q = \frac{r}{x} = \frac{1-6|d|^2+|d|^4}{4y_h(1-|d|^2)}$$

5. Application Example and Discussion

In oscillator theory, the active circuit must exhibit an infinite value of the reflection coefficient at the desired frequency. Surely, the use of a 2D Smith chart based on Euclidean geometry is unattainable to visualize the phenomenon (as seen in Figure 11).

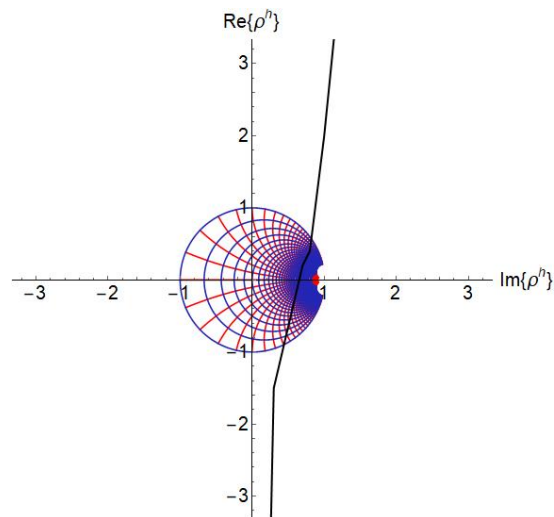


Figure 11. Input impedance (in black) of a microwave oscillator based on an Infineon bipolar transistor send towards infinity in the Euclidean geometry of the 2D Smith chart.

In the hyperbolic reflection plane, governed by Non-Euclidean geometry [16] this phenomenon is easy to be seen in Figure 12a, while in Figure 12b on the 3D Smith chart.

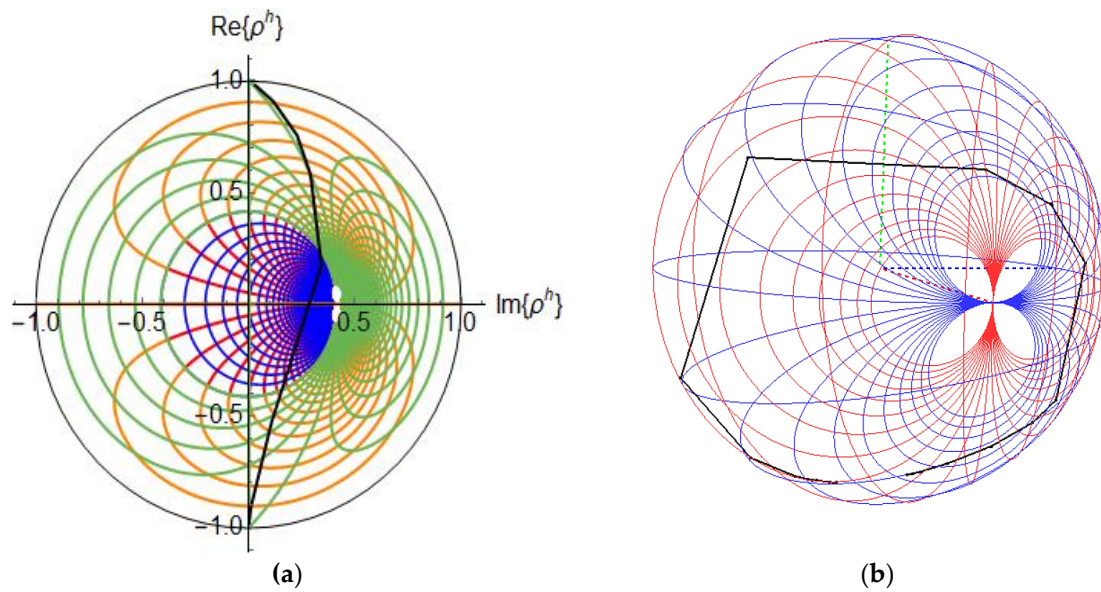


Figure 12. (a) Input impedance (in black) of a microwave oscillator based on an Infineon bipolar transistor is approaching infinity (unit circle) $|\rho| = \infty \Leftrightarrow |\rho^h| = 1$ on the hyperbolic Smith chart. Thus, its behaviour (capacitive/ inductive approach of infinity) can be always easily seen on this later hyperbolic Smith chart; (b) 3D Smith chart representation of the input impedance (through a few discrete frequency points).

The hyperbolic Smith chart (whose main properties are summarized in Table 2) maps the infinite mismatch into the contour of the unit circle, thus if one would use a new vocabulary when passing from one geometry to another [18] one can translate infinite reflection coefficient (Smith chart) into the proper representation (Table 3).

Table 2. Comparative capabilities of the Hyperbolic Smith chart.

Comparative Capabilities	Hyperbolic Smith Chart
Positive resistance	Inside the 0.414 radius circle
Negative resistance	Between the 0.414 radius circle and unit circle
Perfect match	Origin
$ \rho = \infty$	Unit circle
Inductive	Above x_h axes
Capacitive	Bellow x_h axes
r, x, g, b constant	Quartic curves and 0.414 radius circle circumference
Purely resistive	Ox_h axes

Table 3. Vocabulary.

Chart	Geometry	$ \rho = \infty$
Smith Chart	2D Euclidean	Not usable
Extended 2 Smith chart	2D Euclidean	unending
3D Smith chart	Inversive, spherical	South pole
Hyperbolic Smith chart	hyperbolic	Contour of the unit circle

6. Conclusions

We have presented the geometric properties of the Smith chart, 3D Smith chart and Hyperbolic Smith chart by means of inversive geometry and hyperbolic geometry.

The infinite magnitude of the reflection coefficient is mapped by these charts (drawn when applied to the grid of the normalized impedance plane) into different locations: infinity on the 2D Smith chart, South pole on the 3D Smith chart and contour of the unit disc for the Hyperbolic Smith chart.

Further we presented for the first time the equations of the Hyperbolic Smith chart, diagram which was previously just intuitively drawn.

The infinity treatment exceeds the classical electrical engineering books and is based on applied pure mathematics (and not engineering manipulations of equations).

In the future, the topology of the 3D Smith chart in particular can be expanded to deal with more complex phenomenon such as phase change materials [21,22] where their physical properties vary a lot as frequency or temperature changes. The compact (spherical) representation of its reflection coefficients on its surface leaves the space surrounding it free to be used for visualizing other parameters by employing 3D Euclidean geometry or space filling concepts where the notion of infinity may be treated differently.

Author Contributions: A.A.M. proposed the format of the article and introduced the concepts of 3D Smith chart and hyperbolic Smith chart. M.J.P-P and E.S-C developed the further new mathematical properties (equations) (13)–(24) of the hyperbolic Smith chart starting from A.A.M initial concept. A.M., V.A. and F.M. developed the 3D Smith chart Java implementation and revised and arranged the paper, A.I. supervised the work and proposed the further development of the 3D chart to deal with further multi-parameter problems by means of other geometries.

Funding: This research was partially funded by DGCYT grant number MTM2015-64013-P.

Acknowledgments: A.A.M. would like to thank to Lola Demchenko-Gonzalez for help with Figure 5.

Conflicts of Interest: The authors declare no conflict of interest.

References

- Smith, P.H. Transmission-line calculator. *Electronics* **1939**, *12*, 29–31.
- Smith, P.H. *Electronic Applications of the Smith Chart*; McGraw-Hill Book Company: New York, NY, USA, 1969.
- Fikioris, G. Analytical studies supplementing the Smith Chart. *IEEE Trans. Educ.* **2004**, *47*, 261–268. [[CrossRef](#)]
- Trueman, C.W. Interactive transmission line computer program for undergraduate teaching. *IEEE Trans. Educ.* **2000**, *43*, 1–14. [[CrossRef](#)]
- Huang, C.L.; Pang, Y.H.; Tsai, K.L. Web-based Smith Chart learning helper. A guessing game for quarter-wavelength transformer. In Proceedings of the 2013 IEEE International Conference on Teaching, Assessment and Learning for Engineering (TALE), Bali Dynasty Resort, Kuta, Indonesia, 26–29 August 2013; pp. 410–413.
- Graham, P.J.; Distler, R.J. Use of the Smith Chart with complex characteristic impedance. *IEEE Trans. Educ.* **1968**, *11*, 144–146. [[CrossRef](#)]
- Muller, A.A.; Soto, P.; Dascalu, D.; Neculoiu, D.; Boria, V.E. A 3-D Smith Chart based on the riemann sphere for active and passive microwave circuits. *IEEE Microw. Wirel. Compon. Lett.* **2011**, *21*, 286–288. [[CrossRef](#)]
- Muller, A.A.; Soto, P.; Dascalu, D.; Neculoiu, D.; Boria, V.E. The 3D Smith Chart and its practical applications. *Microw. J.* **2012**, *5*, 64–74.
- Muller, A.A.; Sanabria-Codesal, E.; Moldoveanu, A.; Asavei, V.; Soto, P.; Boria, V.E.; Lucyszyn, S. Apollonius unilateral transducer constant power gain circles on 3D Smith charts. *Electron. Lett.* **2014**, *50*, 1531–1533. [[CrossRef](#)]
- Muller, A.A.; Sanabria-Codesal, E.; Moldoveanu, A.; Asavei, V.; Lucyszyn, S. Extended capabilities of the 3-D Smith Chart with group delay and resonator quality factor. *IEEE Trans. Microw. Theory Tech.* **2017**, *65*, 10–19. [[CrossRef](#)]
- Bocher, M. Infinite regions of various geometries. *Bull. Am. Math. Soc.* **1913**, *20*, 185–200. [[CrossRef](#)]
- Gupta, M. Escher's art, Smith chart, and hyperbolic geometry. *IEEE Microw. Mag.* **2006**, *7*, 66–76. [[CrossRef](#)]
- Muller, A.A.; Sanabria-Codesal, E. A hyperbolic compact generalized Smith Chart. *Microw. J.* **2016**, *59*, 90–94.
- Muller, A.A.; Sanabria-Codesal, E.; Moldoveanu, A.; Asavei, V.; Dascalu, D. Two compact Smith Charts: The 3D Smith Chart and a hyperbolic disc model of the generalized infinite Smith Chart. *Rom. J. Inf. Sci. Technol.* **2016**, *19*, 166–174.

15. Brannan, D.A.; Esplen, M.F.; Gray, J.J. *Geometry*; Cambridge University Press: Cambridge, UK, 1999.
16. Iversen, B. *Hyperbolic Geometry, London Mathematical Society Student Texts 25*; Cambridge University Press: New York, NY, USA, 2008.
17. Hvidsten, M. *Exploring Geometry*; CRC Press: Boca Raton, FL, USA, 2016.
18. Poincare, H. *Science and Hypothesis*; Dover Publications: New York, NY, USA, 1912.
19. White, J.F. *High Frequency Techniques: An Introduction to RF and Microwave Engineering*; John Wiley & Sons: New York, NY, USA, 2004.
20. 3D Smith Chart. Available online: <http://www.3dsmithchart.com> (accessed on 3 September 2018).
21. Casu, E.A.; Muller, A.A.; Fernandez-Bolanos, M.; Fumarola, A.; Krammer, A.; Schuler, A.; Ionescu, A.M. Vanadium oxide bandstop tunable filter for Ka Frequency Bands based on a novel reconfigurable spiral shape defected ground plane CPW. *IEEE Access* **2018**, *6*, 12206–12212. [[CrossRef](#)]
22. Phase Change H2020 Project. Available online: <https://phasechange-switch.org/> (accessed on 3 September 2018).



© 2018 by the authors. Licensee MDPI, Basel, Switzerland. This article is an open access article distributed under the terms and conditions of the Creative Commons Attribution (CC BY) license (<http://creativecommons.org/licenses/by/4.0/>).